

Proceedings

Fabrication Methods for High-Performance Miniature Disks of Terfenol-D for Energy Harvesting [†]

Valentin Issindou ^{1,*}, B. Viala ¹, L. Gimeno ², O. Cugat ², C. Rado ^{3,4} and S. Bouat ⁵

¹ CEA, LETI, MINATEC Campus, F-38000 Grenoble, France

² Univ. Grenoble Alpes, CNRS, Grenoble INP, G2Elab, F-38000 Grenoble, France

³ Université Grenoble Alpes, F-38000 Grenoble, France

⁴ CEA, LITEN, DTNM, SERE, LMA, F-38054 Grenoble, France

⁵ ENERBEE, 7 parvis Louis Néel, CS 20050, 38040 Grenoble, France

* Correspondence: valentin.issindou@cea.fr; Tel.: +33-695-741-664

[†] Presented at the Eurosensors 2017 Conference, Paris, France, 3–6 September 2017.

Published: 8 August 2017

Abstract: In this paper, we compare different techniques to manufacture high-performance miniature disks of Terfenol-D aiming at self-powered IoT sensors. To reach large in-plane magnetostriction while maintaining low driving field, microstructure engineering is essential. This work covers monocrystalline, polycrystalline and hot-pressed powder materials whose performances are analyzed. A “performance phase diagram per technique” is reported at the end.

Keywords: magnetostriction; energy; harvesting; multiferroic; sintering; SPS

1. Introduction

Terfenol-D offers the highest known room-temperature saturation magnetostriction strain (λ_{sat}) with practical driving fields. It was originally engineered for sonar transducers, actuators, linear motors and torque sensors, and used in the form of high-purity monocrystalline rods with centimeter dimensions. Prices remain high and machining difficult and production has slowed sharply because of substituting piezoelectric materials. Today Terfenol-D is experiencing a renewal with high performance multiferroic composite materials combining high magnetostriction and piezoelectric constants. Composites of Terfenol-D and PZT can produce exploitable amounts of electrical energy to supply low-power electronics [1,2]. Terfenol-D manufacturing techniques must meet new criteria, i.e., miniaturization and low cost, while maintaining high strain performance.

2. Experimental

This work is focused on the production of millimeter disks of Terfenol-D (diameter 6 mm, thickness 1 mm) whose in-plane properties (microstructural and magnetic) were measured. Four series of disks were prepared. They were either cut from commercial centimeter monocrystalline Terfenol-D rods and cast polycrystalline ingots, or sintered from commercial powders (0–38 μm diameter). We used two hot press techniques at 1075 °C based on conventional heating and SPS (Spark Plasma Sintering), respectively. Magnetic in-plane characterizations were performed using a vibrating sample magnetometer with 360° angular excursion, radial saturation magnetostriction strain were measured at 2 T with the capacitance method, optical metallography, SEM observations and density measurements were performed.

3. Results

Differences in structural appearance for the four disks series are shown in Figure 1. On Figure 1a, optical metallography revealed the surface of cut single-crystal disks. Samples are generally twinned exhibiting a fine lamellar structure with twin boundaries, being the result of a dendritic growth [3]. Θ - 2Θ X-ray diffraction (not shown here) indicates that the normal disk direction is [112] which is the natural Terfenol-D growth direction. Figure 1b shows results for a disk cut from cast polycrystalline alloy. It reveals a polycrystalline structure consisting in a mixture of [112]-oriented grains and randomly-oriented grains. Figure 1c,d show cross-sectional SEM pictures of sintered samples. Unlike the first two series, hot-pressed powder materials are not dense compare to bulk. Density measurements indicate 70% of the theoretical density with an average porosity size of $\sim 10 \mu\text{m}$ for conventional annealing (Figure 1c) and 90% and $\sim 2 \mu\text{m}$ for SPS (Figure 1d).

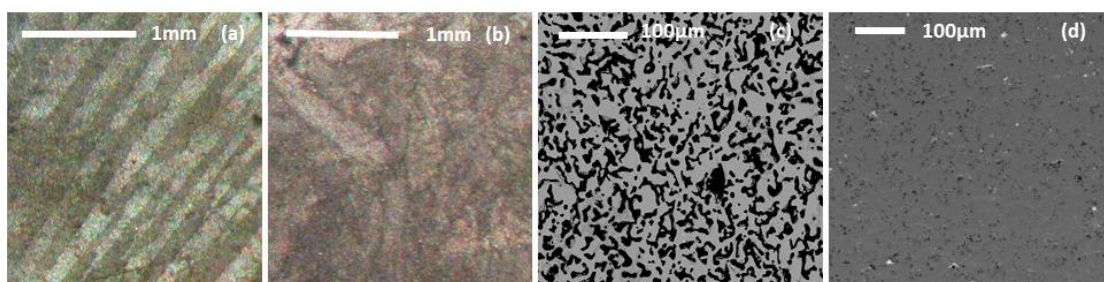


Figure 1. Structural images of miniature disks of Terfenol-D: cut from single crystals rod. (a) cut from cast polycrystalline ingot; (b)-optical images, and hot-pressed from powder (0–38 μm) with conventional heating; (c) and SPS (Spark Plasma Sintering); (d)-SEM images.

Figure 2 shows typical in-plane hysteresis loops of single crystal disks with different applied magnetic field azimuthal angle. We observe that the approach to saturation depends on the angle which reveals the magnetocrystalline anisotropy of the sample. To make comparing series of samples easier, we introduce two reduced quantities defined from hysteresis loops: the magnetization squareness ratio at 0.2T ($SQR_{0.2T}$) and the anisotropy ratio k .

$$SQR_{0.2T} = \frac{M_{0.2T}}{M_{sat}} \quad (1)$$

$$k = \frac{SQR_{0.2T} \max}{SQR_{0.2T} \min} \quad (2)$$

$SQR_{0.2T}$ reflects the ease with which the material saturates for a given applied field angle. The values close to unity correspond to easy axes and the values far from unity to hard axes. The ratio k is used to quantify the degree of anisotropy of the samples.

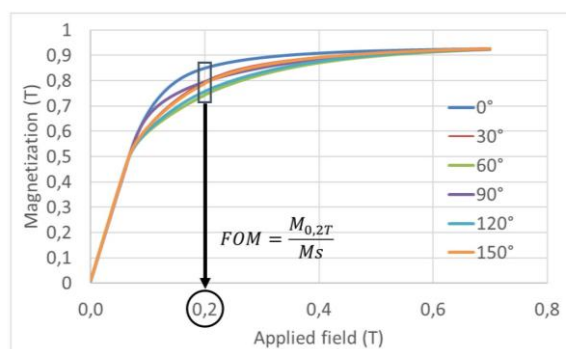


Figure 2. Example of in-plane hysteresis loops (upper branch only) at different azimuthal applied field angles for monocrystalline Terfenol-D disk.

Typical polar plots with $SQR_{0.2T}$ are shown in Figure 3 for monocrystalline, polycrystalline and sintered samples. For disks cut from single crystals, one can identify expected easy axes at 0° and 90° and hard axis at 39° and 129° . This is consistent with the $[112]$ orientation of the samples. For disks cut from cast materials, variation of $SQR_{0.2T}$ over the angle is weaker indicating lowered anisotropy which is consistent with the observation of partially disoriented grains. Finally, results for hot-pressed powder materials are circular (isotropic) which is expected for randomly distributed grains. Lower radii for polycrystalline and sintered samples indicate higher driving fields to reach the saturation due to internal demagnetizing fields (grain boundaries and porosity).

Figure 4 illustrates the dependence of λ_{sat} with k and reveals three groups of materials: first group on top gathers monocrystalline samples which have both largest anisotropy and magnetostriction. However, a significant disparity was found between disks resulting in a broad dispersion [4]. Second group (middle) corresponds to polycrystalline samples with intermediate k and λ_{sat} values. Third group represents sintered samples with $k = 1$. The line delimiting groups 2 and 3 corresponds to $3/5$ of the saturation magnetostriction of perfect single-crystal considering an ideal random distribution of grains. Polycrystalline samples are above this line because of the presence of residual $[112]$ -oriented grains. Sintered samples are below this line because of traces of oxidation which strongly impinge saturation magnetization and magnetostriction.

When looking in more detail at group 3, the highest point corresponds to SPS with which the oxidation is most limited. The lower points go with conventional annealing with which the low magnetostriction $R_{12}Fe_3O_2$ phase preferably forms from porosities as illustrated on Figure 5. Therefore, SPS technique takes advantage over conventional annealing for the production of intermediate high performance sintered Terfenol-D material as it reduces internal porosities and oxidation. The performance can then reach that of cast alloy being in addition completely isotropic.

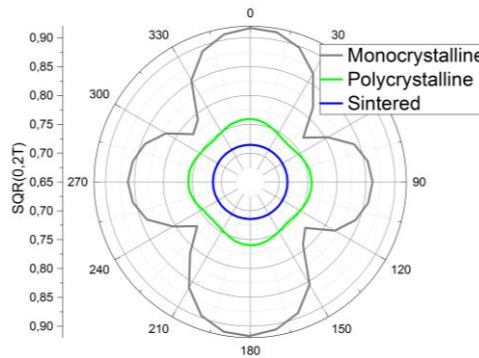


Figure 3. Example of polar plots for monocrystalline, polycrystalline and sintered disks.

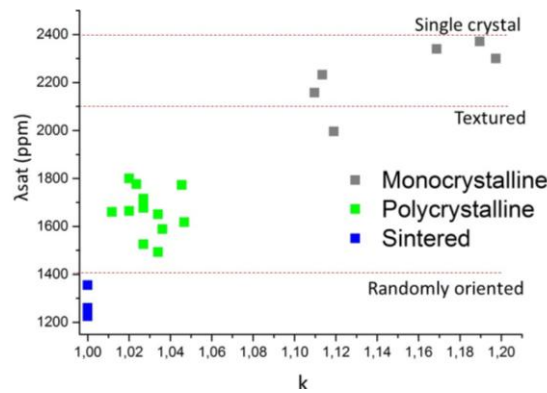


Figure 4. Dependence of the saturation magnetostriction λ_{sat} with the magnetic anisotropy ratio k for monocrystalline, polycrystalline and sintered samples.

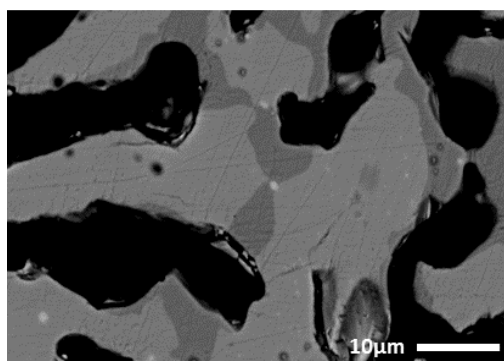


Figure 5. $R_{12}Fe_3O_2$ phase observed by SEM (dark grey areas) on sintered Terfenol-D with conventional annealing at 1075 °C.

Figure 6 illustrates the obtained “performance phase diagram per technique”. For applications, attention is focused on the couple $\lambda_{sat}, H_{sat}^{90\%}$ (practical drive field to reach 90% of λ_{sat}). Our results (in blue) complement those of the literature (in black) [5–7]. As expected, Terfenol-D single crystals remain the most efficient material located at the top left of the diagram. However, the best performance with miniature disks is obtained with a selection of sorted samples. The diagram reveals the very broad dispersion with unsorted single crystal disks approaching the intermediate performance materials. This central area (new) is occupied by disks of cast polycrystalline materials which have been little used before. The area for sintered materials is shifted on the bottom right of the diagram. Hot-pressed powder materials are further penalized by higher driving fields due to residual porosity and oxidation. In this work, we show that SPS technique may bring them back close to the middle with reducing these defects. More, sintered materials (not oriented) are isotropic.

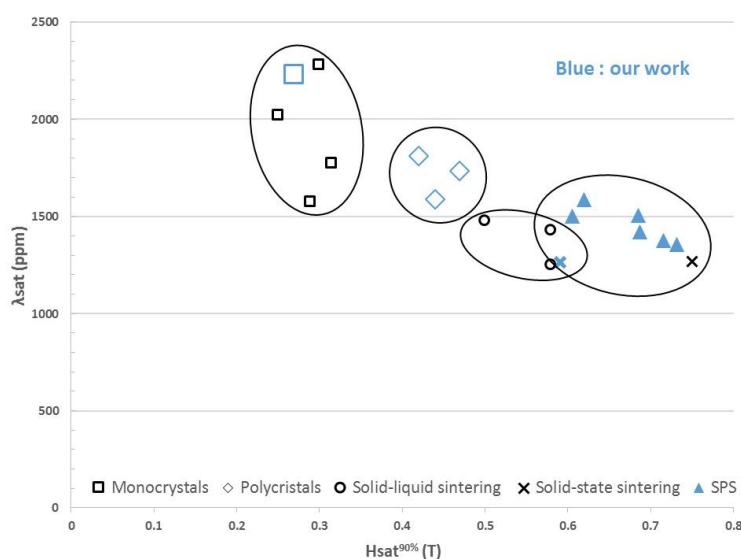


Figure 6. “Performance phase diagram per technique” as λ_{sat} vs. $H_{sat}^{90\%}$ (field required to reach 90% of λ_{sat}). Blue symbols are our work, black symbols are from literature.

4. Conclusions

Finally, we conclude that miniature disks of Terfenol-D sintered from powders or cut from cast polycrystalline alloys are able to produce exploitable amounts of electrical energy for low power IoT sensors under practically reachable magnetic fields (~0.6 T). Moreover, we show that they may have a much less dispersed production and sensitively cheaper than those cut from high performance single crystal rods. Additionally, it is possible to optimize the manufacturing process for the hot-pressed material with SPS to reach even higher density, lower practical field and higher intermediate performances at the end.

Acknowledgments: We would like to thank the Direction Générale de l'Armement for its financial support.

Conflicts of Interest: The authors declare no conflict of interest.

References

1. Lafont, T.; Gimeno, L.; Delamare, J.; Lebedev, G.A.; Zakharov, D.I.; Viala, B.; Cugat, O.; Galopin, N.; Garbuio, L.; Geoffroy, O. Magnetostrictive-piezoelectric composite structures for energy harvesting. *J. Micromech. Microeng.* **2012**, *22*, 094009.
2. Available online: <http://www.enerbee.fr/> (accessed on 15 July 2017).
3. Verhoeven, J.D.; Gibson, E.D.; McMasters, O.D.; Baker, H.H. The growth of single crystal Terfenol-D crystals. *Metall. Trans. A* **1987**, *18*, 223–231.
4. ACTUATOR—International Conference and Exhibition on new Actuators and Drive Systems. Available online: <http://www.actuator.de/programme/2016-06-14/A3/86> (accessed on 15 July 2017).
5. Teter, J.P.; Clark, A.E.; McMasters, O.D. Anisotropic magnetostriction in Tb_{0.27}Dy_{0.73}Fe_{1.95}. *J. Appl. Phys.* **1987**, *61*, 3787–3789.
6. Mei, W.; Okane, T.; Umeda, T. Magnetostriction of Tb–Dy–Fe crystals. *J. Appl. Phys.* **1998**, *84*, 6208–6216.
7. Malekzadeh, M. *Powder Metallurgical Processing of Magnetostrictive Materials Based on Rare Earth-Iron Intermetallic Compounds*; Lawrence Berkeley National Laboratory: Berkeley, CA, USA, 1978.



© 2017 by the authors. Licensee MDPI, Basel, Switzerland. This article is an open access article distributed under the terms and conditions of the Creative Commons Attribution (CC BY) license (<http://creativecommons.org/licenses/by/4.0/>)